WEP
Warwick
Evans
Publishing

International Journal of Mechanical and Electrical Engineering

ISSN: 3005-9615 (Print), ISSN: 3005-7132 (Online) | Volume 8, Number 1, Year 2026
DOI: https://doi.org/10.62051/ijmee.v8n1.14
Journal homepage: https://wepub.org/index.php/IJMEE/index

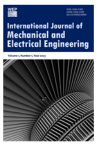

The Construction, Preparation and Characterization of VC Coating

Yue Chen

School of mechanical engineering, Tianjin University of Technology and Education, Tianjin, 300222, China

ABSTRACT

With the increasing attention of human to resource conservation and environmental protection, green dry cutting technology has been widely concerned. In the dry cutting process, if the protective coating with self-lubricating function is applied on the surface of the tool, the coefficient of friction can be reduced, the cutting heat can be reduced, the temperature of the cutting zone can be effectively reduced, the anti-wear and high-temperature resistance of the tool can be enhanced, the tool chipping can be inhibited, the service life can be prolonged, the processing efficiency can also be improved, and the surface processing quality of the workpiece can be improved. However, for high-hardness coatings, as the temperature rises, the tool will often appear to adhere to oxidation, which requires the use of the coating itself to produce a lubricating effect, so as to reduce the occurrence of such situations. In addition, V reacts with oxygen during friction to form Magnéli phase oxide V_2O_5 with lubricating effect to achieve a friction reduction effect. In this paper, the crystal structure, commonly used preparation methods, and performance characterization of vanadium carbide (VC) coatings, a self-lubricating coating with high hardness and low friction in a wide temperature range are introduced.

KEYWORDS

VC Coating; Green Dry Cutting Technology; Crystal Structure; Preparation Methods; Performance Characterization.

1. INTRODUCTION

At present, the preparation technology of hard coatings has been highly sophisticated and is widely applied in various fields [1-3]. However, hard coatings exhibit an extremely high friction coefficient. During dry cutting, severe friction induced thereby gives rise to excessive cutting force and elevated cutting temperature, which compromises the service life of cutting tools, the surface quality of machined workpieces, and machining efficiency [4]. In addition, grease lubrication and cutting fluids are not applicable in special scenarios subject to environmental factors. The volatilization and thermal degradation of grease under high-temperature conditions constitute the primary obstacles to their widespread application. Therefore, depositing self-lubricating hard coatings on workpiece surfaces is an effective approach to addressing this problem. When self-lubricating coatings are applied to cutting tool surfaces, the frictional action during cutting induces the formation of lubricious oxide films on the coatings. These films reduce friction between the tool and the workpiece, effectively lowering cutting temperature and cutting force, mitigating tool wear and built-up edge formation, and ultimately achieving the goal of extending tool service life. For these reasons, such coatings are regarded as the most ideal lubricating materials [5, 6].

Compared with nitrides, vanadium carbide possesses a higher hardness and also exhibits excellent comprehensive mechanical properties. However, transition metal carbides generally have relatively complex phase compositions and are rather difficult to prepare, which has impeded the development of these promising coating materials. As one of the hardest transition metal carbides, vanadium carbide also boasts many outstanding properties. For instance, the vanadium pentoxide (V_2O_5) formed on its surface during service can significantly reduce the cutting resistance of tools through its self-lubricating effect[7-8]. Thiis paper mainly introduces the crystal structure, common preparation methods, as well as the characterization and performance testing of vanadium carbide (VC) coatings.

2. THE CRYSTAL STRUCTURE OF VC COATINGS

Vanadium carbide (VC) features a typical NaCl-type crystal structure, as illustrated in Figure 1. In the VC crystal lattice, each vanadium (V) atom is surrounded by six carbon (C) atoms, and vice versa. The V and C atoms extend in all spatial directions following this arrangement, thereby forming the vanadium carbide crystal. VC crystallizes in the cubic system, where V atoms adopt a face-centered cubic (FCC) close-packed structure, and C atoms fill the octahedral interstitial sites. In addition, both types of atoms have a coordination number of 6.

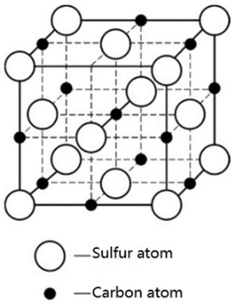

Figure 1. Crystal Structure of VC

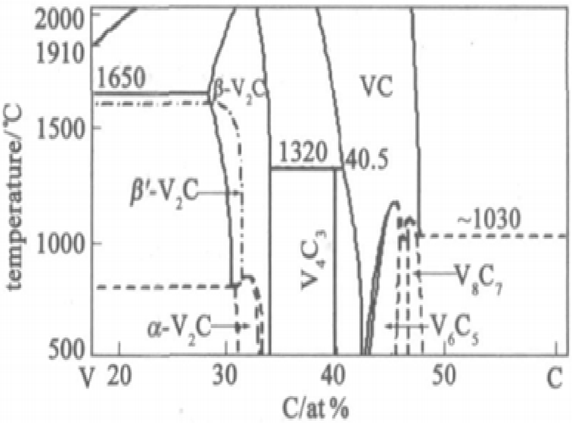

Figure 2. V-C Phase Diagram[10]

In addition, the crystal structures of VC coatings vary with their different carbon contents. Li et al [9] fabricated VC films with carbon contents of 27.07 %, 48.76 %, 54.94 %, 66.42 % and 81.04 %, respectively. Combined with the analysis of the V-C phase diagram[10] (as shown in Figure 2), the experimental results demonstrated that when the carbon content of vanadium carbide in the VC film was 27.07 %, the atomic ratio of V to C in the film was approximately 2:1, with the corresponding phase composition being V_2C+V. V_2C exists in two structural forms: α-V_2C with an orthorhombic structure (a=0.4567 nm, b=0.5744 nm, c=0.5026 nm) and β-V_2C with a hexagonal structure (a=0.2904 nm, c=0.4576 nm). When the carbon content ranged from 48.76 % to 54.94 %, the atomic ratio of V to C was about 1:1, and the phase composition of the film was extremely complex at this stage. The corresponding phases included VC, or V_8C_7 and even V_6C_5 generated by low-temperature ordering, or carbon phases formed within VC, thus resulting in a multiphase structure. When the carbon content exceeded 80 %, the VC film was composed of two phases, namely VC and C.

3. PREPARATION METHODS OF VC COATINGS

At present, researchers have fabricated VC coatings via various techniques, including arc ion plating, thermal reactive diffusion, pulsed laser deposition, magnetron sputtering, and electron beam evaporation.

3.1. Arc Ion Plating (AIP) Technology

Ion plating technology (AIP) is a novel coating deposition technique developed on the basis of vacuum evaporation and vacuum sputtering. The working principle of AIP is as follows: the furnace body serves as the anode and the target material as the cathode to trigger arc discharge; one or more arc spots are formed on the surface of the cathode target. Driven by arc discharge, the cathode target is evaporated and ionized into plasma, which is then deposited onto the substrate surface under the action of a magnetic field. Arc ion plating boasts the advantages of high deposition rate, excellent throwing power, capability for large-area deposition, flexible target selection, and easy disassembly. Moreover, the coatings prepared by this technique are dense, uniform, and of high quality [11-13]. Wang Chongyang[14] adopt high-purity vanadium targets (99.5 %), and high-purity acetylene (C_2H_2, 99.99 %) gas was introduced to supply carbon ions for depositing VC coatings via arc ion plating at a constant temperature of 400 °C. The results demonstrated that with the increase in carbon content, the content of the hard VC phase increased and the hardness of the VC coating accordingly rose, followed by a decrease due to the accumulation of amorphous carbon, as illustrated in Figure 3. The coating achieved the maximum hardness and elastic modulus of 28.6 GPa and 394.0 GPa, respectively, along with a peak critical load of 64 N, when the carbon content reached 31.22 at.%.

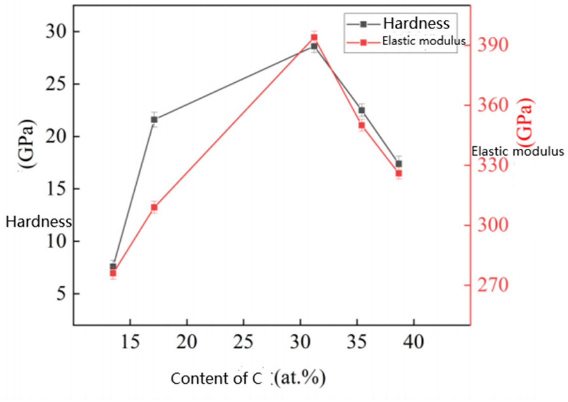

Figure 3. Hardness and Modulus of Elasticity of VC Coatings with Different C Contents [14]

3.2. Thermal Reactive Diffusion Technology

Thermal Reactive Diffusion (TRD) technology was first reported by Arai in the 1970s and was then named the Toyota Diffusion Process. This process is carried out in a molten borax salt bath at a temperature of approximately 1000 °C. During the TRD process, the formation and growth of different coatings at the interface between the substrate and the surface coating are governed by diffusion laws. Compared with other coating techniques such as physical vapor deposition (PVD) and chemical vapor deposition (CVD), TRD technology enables the deposition of metal and nitride coatings at low cost with relatively simple equipment, and is also environmentally friendly[15, 16]. Aghaie-Khafri et al [17] obtained hard, dense and smooth vanadium carbide coatings on the surface of die steel substrates using powder mixtures composed of ferrovanadium, ammonium chloride, alumina and naphthalene at different temperatures. The results showed that in friction and wear tests, vanadium carbide-coated steel exhibited superior wear resistance compared with uncoated steel. The hardness of the coatings was approximately four times that of the uncoated steel, as illustrated in Figure 4.

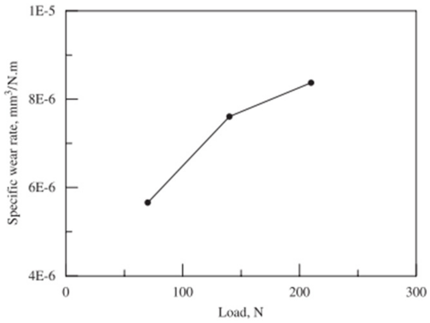

Figure 4. Specific Wear Rate of Vanadium Carbide-coated Steel at 1050 °C and 3 h as a Function of Wear Load [17]

3.3. Pulsed Laser Deposition Technology

Pulsed laser deposition (PLD) is a thin-film fabrication process that relies heavily on laser technology. This technique offers several advantages, including high deposition rate, low required substrate temperature, excellent composition retention, broad applicability, and ease of cleaning. However, PLD also has certain limitations, for instance, large particulate droplets tend to form during the deposition process, which impairs the surface quality and flatness of the resultant thin films[18]. Teghil et al[19] employed ultrashort pulsed laser deposition technology, using a frequency-doubled Nd:glass laser with a pulse duration of 250 fs to ablate a VC target, and deposited vanadium carbide films on silicon substrates. They further compared these results with those obtained on tantalum carbide substrates. The findings indicated that PLD of VC via ultrashort pulsed laser yielded outcomes consistent with those of tantalum carbide; however, the ablation-deposition mechanism remains unclear.

3.4. Magnetron Sputtering Technology

Magnetron sputtering is a technique developed on the basis of conventional direct current (radio frequency) sputtering. Early-stage direct current (radio frequency) sputtering realized thin-film deposition by bombarding target materials with ions generated by glow discharge. However, this sputtering method suffered from low deposition rates and high operating pressure. To improve the deposition rate and reduce the operating pressure, a magnetic field was applied to the back of the target material, which gave rise to the original magnetron sputtering technology[20]. Aouni et al[21] prepared a series of vanadium carbide films with different carbon contents via reactive sputtering using vanadium targets and methane (CH_4) gas. They found that the partial pressure of the reactive gas exerted a significant influence on the composition and microstructure of the vanadium carbide films. With the increase in CH_4 partial pressure (ranging from 3 % to 15 %), single-phase or multiphase vanadium carbide films—including V, V_2C, VC, and VC/C composites—could be obtained depending on the carbon content. Magnetron sputtering exhibits the advantages of high deposition efficiency, high target utilization rate, and improved surface quality of sputtered coatings or films. However, this technique is not suitable for the sputtering of ferromagnetic materials.

3.5. Electron Beam Evaporation

Electron beam evaporation (EBE) is a method in which electron beams are directly used to evaporate target materials under vacuum conditions, causing the materials to vaporize, deposit onto the substrate, and condense into thin films. Its working principle is as follows: the evaporation material is placed in an evaporation source inside a vacuum chamber; under high-vacuum conditions, an electric field is applied to the electrons emitted by the hot cathode, converting them into a high-energy-density electron beam. The electron beam directly bombards the coating material, heating it to vaporize and evaporate before depositing and condensing into a film on the substrate [22]. Frerro et al [23] obtained single-phase VC films with an NaCl-type structure via electron beam evaporation using VC targets, and the films exhibited a high hardness of 25 GPa. Electron beam evaporation enables the evaporation of high-melting-point materials and boasts advantages such as high evaporation rate and high product quality, thus being widely applicable to the preparation of high-purity films. However, electron beam evaporation equipment is relatively complex and expensive.

4. PERFORMANCE CHARACTERIZATION OF VC COATINGS

4.1. Phase Composition of the Coating

The phase composition of the coating can be characterized by various diffraction techniques, among which the most commonly used ones include electron diffraction and X-ray diffraction (XRD) [24]. The X-ray diffraction technique was adopted in this laboratory to characterize the phase composition of the coatings. The instrument operated under the following parameters: Cu target X-ray tube, 20 kw, voltage ≤ 40 kV, current ≤ 40 mA. Its working principle is that diffraction occurs when X-rays irradiate the crystals, and the continuous superposition of diffracted waves enhances the intensity of the rays in specific directions while weakening it in other directions. The crystal structure can be determined by analyzing the different diffraction patterns obtained. The X-ray diffraction angle ranged from 20° to 90°, with a scanning step size of 0.02°. The detector had a maximum count rate of 1×10^9 cps, a linear range of 4×10^7 cps, and an energy resolution better than 680 eV, making it suitable for the detection of both coating samples and bulk solids.

4.2. Microstructure Morphology and Composition of the Coating

There are numerous methods for characterizing the microstructure and morphology of coatings, with the commonly used ones including various microscopes such as optical microscopy (OM), scanning electron microscopy (SEM), transmission electron microscopy (TEM), scanning tunneling microscopy (STM), and atomic force microscopy (AFM). In this laboratory, scanning electron microscopy (SEM) is mainly employed to observe the microstructure, morphology and composition of the coatings. Scanning electron microscopy (SEM) generates images by modulating various physical signals excited when a focused electron beam scans the surface of the sample. Combined with other analytical instruments, modern SEM can not only characterize morphological features, but also analyze multiple microstructural pieces of information such as micro-area composition and crystal structure, making it one of the most direct techniques for material structure research[25-26].

In this paper, the surface morphology, cross-sectional morphology, and composition of the coatings were all characterized using a field emission scanning electron microscope (FE-SEM, Hitachi SU8010 model). The electron microscope scans the sample surface with a highly focused electron beam in a raster pattern, and clear micro-morphologies are obtained by collecting and processing the secondary electrons generated from the interaction between the electron beam and the sample. This SEM features a continuous magnification range of 200,000–2,300,000×, along with advantages such as a large field of view and stereoscopic imaging. Furthermore, equipped with an X-ray energy dispersive spectrometer (EDS), the SEM enables simultaneous observation of the coating's microstructural morphology and analysis of its composition, which is of great significance for micro-morphology characterization.

4.3. Hardness and Elastic Modulus of the Coating

Hardness is defined as the ability of a metallic material's surface to resist indentation by other hard objects. It is an important indicator for evaluating the hardness and softness of metallic materials. The most commonly used method for hardness measurement is the indentation method. In engineering applications, the widely adopted hardness testing standards include Brinell hardness, Rockwell hardness, and Vickers hardness [27]. In this laboratory, the hardness of the coatings was mainly measured using a nanoindentation tester. As an advanced type of instrument for testing the surface mechanical properties of materials, the nanoindentation tester is equipped with high-resolution actuators and sensors, which can control and monitor the indenter's indentation into and withdrawal from the material. It enables high-resolution continuous measurement of load and displacement, and the contact area can be obtained in real time directly from the load-displacement curve. Thus, it can significantly reduce manual measurement errors, making it highly suitable for measurements with relatively shallow indentation depths [28, 29].

The various properties of hard materials are closely related to their structures, which in turn depend on the materials' phases, chemical compositions, and preparation methods. Currently, the commonly used characterization indicators for hard materials include hardness (H), elastic modulus (E), as well as H/E and H^3/E^{*2}. For hard coatings, the main commonly adopted hardness characterization methods are microhardness testing and indentation testing. In this paper, the hardness and elastic modulus of the coatings were measured using a nanoindentation tester (Model TTX-NHT-3, Anton Paar). Equipped with high-resolution actuators and sensors, this instrument can control and monitor the indenter's indentation into and withdrawal from the coatings, providing high-resolution continuous measurements of applied load and displacement. The contact area can be obtained in real time directly from the load-displacement curve, thus reducing manual measurement errors. The cemented carbide substrates deposited with coatings were fixed on the workbench. Under a high-magnification microscope, the relatively flat and smooth areas of the coatings were selected by adjusting the position of the stage. The test parameters were set as follows: an applied load of 10 mN with a dwell time of 10 s. To eliminate the influence of substrate hardness on coating hardness measurement, the indentation depth of the indenter tip was set to be no more than 1/10 of the coating thickness. A Berkovich diamond indenter was used to apply the load to the coatings. Each sample was tested three times, with ten measurement points selected per test, and the average value was calculated as the final hardness and elastic modulus of the coatings.

4.4. Critical Load of the Coating

The bonding strength between the coating and the substrate is an important indicator for evaluating the mechanical properties of the coating. Common methods for measuring the bonding strength of coatings include the tensile method, bending method, indentation method, scratch-off method, and scratch test method. The bonding capacity between the coating and the substrate determines the duration of the protective effect exerted by the coating on the cutting tool during the machining process, which is of critical importance. In this laboratory, the scratch test method is mainly adopted to measure the bonding strength of hard coatings. Specifically, a stylus with a smooth conical tip is used to scratch across the surface of the hard coating at a constant speed, while the vertical load applied by the indenter is gradually increased. The minimum load that induces cracking of the hard coating is defined as the critical load, which is used to characterize the bonding strength of the coating [30]. The bonding strength between the coating and the substrate was measured using a scratch tester (Model RST-3, Anton Paar). After the scratch test, the load applied when the first crack appeared was defined as L_{c1}, while the load at which the coating completely peeled off from the substrate was denoted as L_{c2}; In this paper, L_{c2} was adopted as the indicator for evaluating the coating-substrate bonding strength. The cemented carbide substrates deposited with coatings were fixed on the workbench. The test parameters were set as follows: a scratch length of 3 mm, a linearly increasing load ranging from 0 to 100 N, and a diamond indenter moving speed of 6 mm/min. Each sample was tested three times, and multiple samples were subjected to the test. The final result of the coating bonding performance was determined by calculating the average value of all test data.

4.5. Tribological Properties of the Coating

The phenomenon of friction and wear is highly complex. There is a wide variety of laboratory equipment and setups for related tests, and the obtained experimental data are strongly dependent on test conditions, which often makes it difficult to conduct direct comparisons. At present, universal tribometers are widely used, which are mainly designed to evaluate the tribological properties of various materials under different conditions of speed, load and temperature.

Friction and wear constitute a significant problem that cannot be ignored for industrial equipment. Globally, approximately 30 % of energy is lost annually due to friction, around 60 % of components fail because of wear, and roughly 50 % of mechanical equipment accidents are caused by excessive wear, resulting in enormous safety hazards and economic losses. Depositing coatings on the surface of workpieces is regarded as an effective method to improve the tribological properties of substrate materials. The commonly used test modes for friction and wear include sliding, rolling, roll-sliding, and reciprocating motion [31]. In this experiment, the tribological properties of the coatings were tested using an Anton Paar THT sliding, surface-contact pin-on-disk high-temperature tribometer. To eliminate the influence of other factors on the friction coefficient, the surfaces of the coatings and the counterparts were cleaned with high-purity ethanol prior to the friction and wear tests. Al_2O_3 balls with a diameter of 6 mm were selected as the friction counterparts, and loads of 2 N or 4 N were applied respectively according to different working conditions. The number of rotation cycles was set at 4000, and the linear rotation speed was fixed at 10 mm/min. For each substrate, three friction tests were conducted at rotation radii of 4 mm, 6 mm, and 8 mm respectively, and two substrates were tested for each type of coating. To ensure the accuracy of the measured friction coefficient, the substrate was not exposed after the friction test. The final friction coefficient of the coating was determined as the average value of the friction coefficients in the running-in stable stage from the six friction tests.

The wear rate is calculated by the formula $K=V/(L\times S)$ [32], where V is the wear volume of the wear scar, L is the applied load, and S is the total friction sliding distance.

5. SUMMARY

Through the introduction of the crystal structure, preparation methods, and performance characterization of VC coatings, the following conclusions can be drawn in this paper.

(1) The VC coating has a typical NaCl-type crystal structure, but low-temperature ordering may lead to the formation of secondary phases, such as V_8C_7 and even V_6C_5.

(2) The preparation methods of VC coatings include arc ion plating, thermal reactive diffusion, pulsed laser deposition, magnetron sputtering, and electron beam evaporation. Among these methods, arc ion plating and magnetron sputtering are the primary techniques for fabricating such coatings. To further improve the efficiency of coating preparation, the two methods can also be combined for application.

(3) In this laboratory, X-ray diffractometry (XRD) was primarily employed to characterize the phase composition of VC coatings; scanning electron microscopy (SEM) was utilized to observe the surface and cross-sectional morphologies of VC coatings; a nanoindentation tester was adopted to measure

the hardness and elastic modulus of VC coatings, a scratch tester was used to determine the bonding strength between VC coatings and the substrate, and a tribometer was applied to evaluate the wear resistance of the coatings.

CONFLICTS OF INTEREST

The authors declare that they have no conflict of interest.

REFERENCES

[1] Syed B, Zhu J, Polcik P, et al. Morphology and microstructure evolution of Ti-50 at.% Al cathodes during cathodic arc deposition of Ti-Al-N coatings[J]. Journal of Applied Physics, 2017, 121(24): 245309.

[2] Azzi M, Benkahoul M, Szpunar J A, et al. Tribological properties of CrSiN-coated 301 stainless steel under wet and dry conditions[J]. Wear, 2009, 267(5-8): 882-889.

[3] Moraes V, Bolvardi H, Kolozsvári S, et al. Thermal stability and mechanical properties of TiAl-BN thin films[J]. International Journal of Refractory Metals and Hard Materials, 2018, 71: 320-324.

[4] Fan Q X, Wang X, Wang Z Q, et al. Milling performance of cemented carbide tools with TiCN coatings[J]. Tool Engineering, 2020, 54(04): 20-23. (in Chinese)

[5] Gardos, Michael N. Magnéli phases of anion-deficient rutile as lubricious oxides. Part I. Tribological behavior of single-crystal and polycrystalline rutile (Ti_nO_{2n-1})[J]. Tribology letters, 2000, 8(2-3): 65-78.

[6] Zabinski J S, Sanders J H, Nainaparampil J, et al. Lubrication using a microstructurally engineered oxide: performance and mechanisms[J]. Tribology Letters, 2000, 8: 103-116.

[7] Mayrhofer P H, Hovsepian Eh P, Mitterer C, et al. Calorimetric evidence for frictional self-adaptation of TiAlN/VN superlattice coatings[J]. Surface and Coatings Technology, 2004, 177: 341-347.

[8] Zhou Z, Rainforth W M, Lewis D B, et al. Oxidation behaviour of nanoscale TiAlN/VN multilayer coatings[J]. Surface Coatings Technology, 2004, 177: 198-203.

[9] Li G Z, Wu X Y, Chen Y H, et al. Microstructure and mechanical properties of vanadium carbide films prepared by reactive magnetron sputtering[J]. Journal of Vacuum Science and Technology, 2009, 29(02): 168-172. (in Chinese)

[10] Okamoto H. Reevaluation of thermodynamic models for phase diagram evaluation[J]. Journal of Phase Equilibria, 1991, 12: 623-643.

[11] Zhao Y H, Shi W B, Liu Z H, et al. Effects of process parameters on arc ion plating deposition[J]. Vacuum, 2018, 55(06): 49-59. (in Chinese)

[12] Wang M L, Cheng W J, Lin G Q. Effects of Arc Current on the Structure and Properties of Ultra-Hard ta-C Films Deposited by Arc Ion Plating[J]. Rare Metal Materials and Engineering, 2022, 51(08): 3095-3102. (in Chinese)

[13] Liu Y, Wang T G, Lin W, et al. Microstructure and properties of the AlCrSi(O)N tool coatings by arc ion plating[J]. Coatings, 2020, 10(9): 841.

[14] Wang C Y. Study on (TiAl)VC Tool Coatings Prepared by Physical Vapor Deposition[D]. Tianjin University of Technology and Education, 2024. (in Chinese)

[15] Kurt B, Küçük Y, Sabri G. Microabrasion Wear Behavior of VC and CrC Coatings Deposited by Thermoreactive Diffusion Technique[J]. Tribology Trans, 2014, 57(2): 345-352.

[16] Ghadi A, Soltanieh M, Saghafian H, et al. Investigation of chromium and vanadium carbide composite coatings on CK45 steel by thermal reactive diffusion[J]. Surface and Coatings technology, 2016, 289: 1-10.

[17] Aghaie-Khafri M, Fazlalipour F. Vanadium carbide coatings on die steel deposited by the thermo-reactive diffusion technique[J]. Journal of Physics and Chemistry of Solids, 2008, 69(10): 2465-2470.

[18] Duan T F. Study on $(Cu,C)Ba_2Ca_3Cu_4O_y$ Films Prepared by Pulsed Laser Deposition and Their Superconducting Properties[D]. Nanjing University, 2020. (in Chinese)

[19] Teghil R, De Bonis A, Galasso A, et al. Nanostructured thin films obtained by ultra-short pulse laser deposition of vanadium carbide[J]. Applied Surface Science, 2009, 255(10): 5220-5223.

[20] Lin Y C, Chen M Z, Kuo C C, et al. Electrical and optical properties of ZnO: Al film prepared on polyethersulfone substrate by RF magnetron sputtering[J]. Colloids and Surfaces A: Physicochemical and Engineering Aspects, 2009, 337(1-3): 52-56.

[21] Liu D. Study on Annealing Process of Fe_3Si Films Prepared by Resistance Thermal Evaporation[D]. Guizhou University, 2017. (in Chinese)

[22] Aouni A, Weisbecker P, Loi T H, et al. Search for New Materials in Sputtered $V_{1-x}C_x$ Films[J]. Thin Solid Films, 2008, 469: 315-321.

[23] Ferro D, Rau J V, Generosi A, et al. Electron beam deposited VC and NbC thin films on titanium: Hardness and energy-dispersive X-ray diffraction study[J]. Surface and Coatings Technology, 2008, 202(10): 2162-2168.

[24] Song G H, Du H, He C L, et al. Hard and Ultra-Hard Coatings: Structure, Properties, Preparation and Characterization[M]. Beijing: Chemical Industry Press, 2007: 236. (in Chinese)

[25] Zhou Y. Materials Analysis Methods[M]. Beijing: China Machine Press, 2005: 309-323. (in Chinese)

[26] Dai D H, Zhou K S, Yuan Z H. Modern Materials Surface Engineering Science[M]. Beijing: Metallurgical Industry Press, 2004: 551-592. (in Chinese)

[27] Tao Y Y, Wang H. Fundamentals of Engineering Materials and Mechanical Manufacturing[M]. Beijing: Chemical Industry Press, 2012: 9. (in Chinese)

[28] Zhang T H. Application and Standardization of Instrumented Nanoindentation Testing Technology[C]. Proceedings of the 2009 Chinese Society of Mechanics Academic Conference, 2009: 237. (in Chinese)

[29] Swain M V, Mencik J. Mechanical property characterization of thin films using spherical tipped indenters[J]. Thin Solid Films. 1994, 253(1-2): 204-211.

[30] Du J, Wang H M, Wang X. Analysis of Influencing Factors on Critical Load for Adhesion Strength Measured by Scratch Test[J]. Surface Technology, 2015, 44(9): 134-139. (in Chinese)

[31] Zhang H, Li G Y, Fu Z, et al. Review of Research Methods for Friction and Wear of Cutting Tools[J]. Manufacturing Technology & Machine Tool, 2015, (01): 142-146. (in Chinese)

[32] Wang T G, Li B S, Zhang J J, et al. Effects of Deposition Temperature on the Structure and Properties of AlCrSiN Coatings Prepared by High-Power Impulse Magnetron Sputtering[J]. Rare Metal Materials and Engineering, 2018, 47(08): 2578-2584. (in Chinese)